

## PWR Core Analysis Using Helios, Serpent and PARCS Codes

Giorgio Baiocco<sup>a</sup>, Alessandro Petruzzi<sup>a</sup>

<sup>a</sup>Nuclear And Industrial Engineering (NINE), Borgo Giannotti 19, Lucca, Italy, [g.baiocco@nineeng.com](mailto:g.baiocco@nineeng.com)

**Abstract** - Lattice physics codes are primarily used to generate cross-section data for nodal codes. In this work the methodology of homogenized constant generation is applied to a small Pressurized Water Reactor (PWR) core, using the deterministic code Helios and the Monte Carlo code Serpent. Subsequently, a 3D analysis of the PWR core is performed with the nodal diffusion code PARCS using the two-group cross section data sets generated by Helios and Serpent. Moreover, a full 3D model of the PWR core is developed using Serpent in order to obtain a reference solution. Several parameters, such as  $k_{eff}$ , axial and radial power are compared and show to be in good agreement.

### 1. INTRODUCTION

Deterministic and Monte Carlo lattice physics codes are currently widely used to produce few-group cross-section data for nodal diffusion codes in order to simulate the neutronics behavior of a reactor core during steady-state and transient operation [1]. Moreover, Monte Carlo codes can be used to obtain a reference solution when experimental data is not available. This is because Monte Carlo techniques can handle complex geometries and continuous energy cross-section data, while deterministic codes work with homogenized multi-group data and simplified geometries.

In this study the deterministic code Helios and the Monte Carlo code Serpent are used to generate two-group cross-section data for a small PWR core. The first objective of this work is to show the consistency between Helios and Serpent results, comparing the two-group diffusion parameters (i.e. cross-sections, diffusion coefficients and assembly discontinuity factors). However, the consistency of Helios and Serpent cross-section data was already shown in [2] and [3] for a typical PWR core. Moreover, the capabilities of Serpent as a lattice physics code were demonstrated in [4] in comparison with CASMO-5M. Here, the cross-section data generated by Helios and Serpent are used with the nodal diffusion code PARCS to perform a 3D analysis of the PWR core. Important core parameters, such as  $k_{eff}$ , and axial and radial power were compared to show the consistency of PARCS results against a 3D Monte Carlo reference modeled with Serpent. Other works have presented successful core analyses using Serpent in conjunction with different nodal codes, such as PARCS, DYN3D and ARES, for PWR [5, 6, 7], BWR [8], SFR [9, 10, 11] and LFR [12].

The paper is structured as follows. Section 2 contains the description of the PWR core considered in the analysis. Section 3 gives an overview of the methods and codes used for the calculation. Section 4 provides a detailed description of the homogenized cross-section generation methodology. Section 5 presents the important core results (i.e.  $k_{eff}$ , axial and radial power) and comparison between PARCS/Helios,

PARCS/Serpent and reference Serpent 3D calculation. Section 6 summarizes the paper and draws conclusion.

### 2. DESCRIPTION OF THE PWR REACTOR CORE

The test case is a small PWR made of 9 fuel assemblies. Each assembly consists of 17x17 array loaded with UO<sub>2</sub> enriched to 4% <sup>235</sup>U. Central assembly contains 20 pins loaded with borosilicate glass as burnable absorber. Pin claddings are made of Zircaloy-4. Control rods are made of Ag-In-Cd. Spacer grids, made by Inconel-718, are located at five different heights in the core, three of them in the active region. The main characteristics of the core are summarized in Table I and Table II. Fig. 1 and Fig. 2 show respectively the radial and axial views of the reactor core.

Table I. Geometrical characteristics of the reactor

Parameter	Value
Pellet diameter, mm	8.50
Insulating pellet diameter, mm	8.47
Burnable absorber pellet diameter, mm	8.35
Control rod pellet diameter, mm	8.35
Clad inner diameter, mm	8.65
Clad outer diameter, mm	9.85
Guide tube inner diameter, mm	11.4
Guide tube outer diameter, mm	12.0
Fuel assembly pitch, mm	220.9
Baffle thickness, mm	19.5
Barrel inner diameter, mm	1026
Barrel outer diameter, mm	1286
Vessel inner diameter, mm	1510
Vessel outer diameter, mm	1710
Active fuel length, mm	781.2
Spacer grids height, mm	38

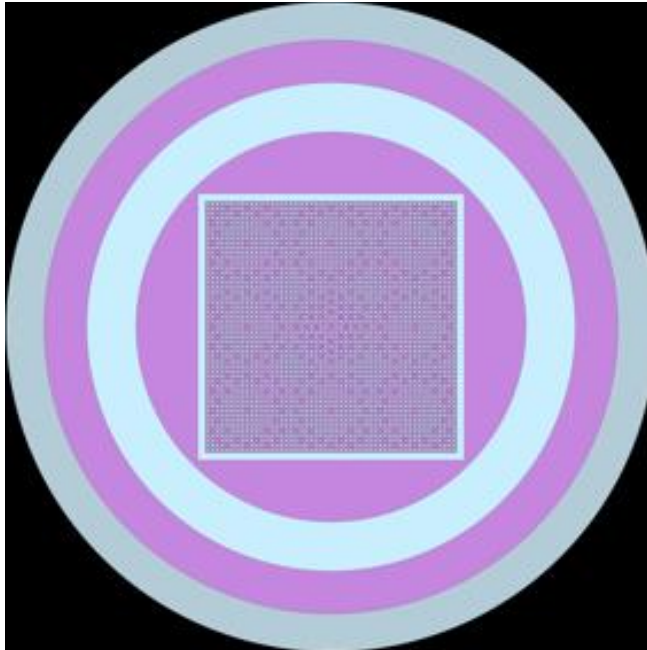


Fig. 1. Radial view of the PWR core, Serpent 3D model.

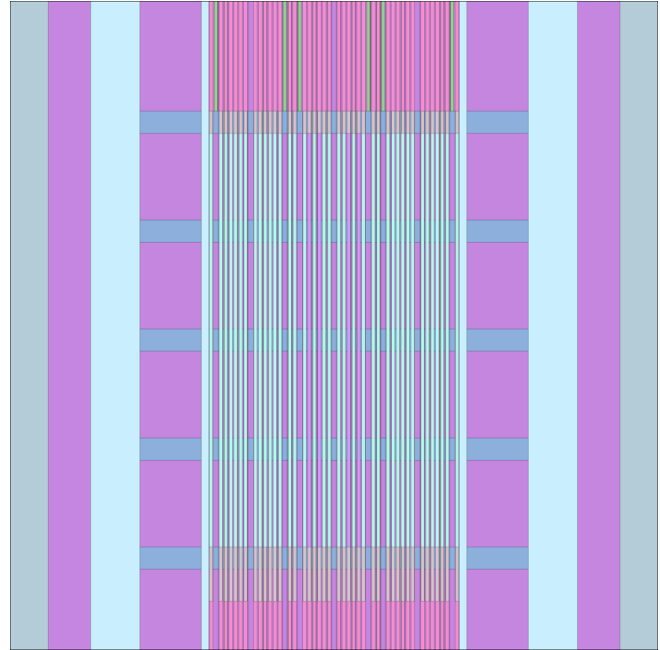


Fig. 2. Axial view of the PWR core, Serpent 3D model.

Table II. Materials in the core

Reactor Part	Material
Fuel	UO <sub>2</sub> 4% enrichment
Gap	Helium
Clad and Guide Tube	Zircaloy-4
Coolant	H <sub>2</sub> O
Burnable absorber	Borosilicate glass
Control rod	Ag-In-Cd
Insulating pellet	Al <sub>2</sub> O <sub>3</sub>
Baffle and Barrel	AISI 347
Pressure vessel	AISI 508
Spacer grid	Inconel-718

### 3. CODES AND METHODS

PARCS is a 3D reactor core simulator which solves the steady-state and time dependent, multi-group neutron diffusion equation [13]. PARCS uses nodal cross-section data generated by lattice physics codes and can be coupled to thermal-hydraulics system codes RELAP5 and TRACE or used as a stand-alone code. In this work the methodology of homogenized constant generation is applied to a small PWR core using the deterministic code Helios and the Monte Carlo code Serpent.

Helios is a commercial neutron and gamma transport and depletion code developed by Studsvik Scandpower [14]. The transport method of Helios is based on current coupling and collision probabilities applied in a 2D unstructured mesh. In this work, Helios is used as a deterministic tool for the two-group cross-section data generation.

Serpent is a 3D continuous energy Monte Carlo reactor physics burn-up calculation code, developed at VTT Technical Research Centre of Finland [15]. In this work Serpent is used as Monte Carlo tool for the two-group cross-section data generation and, moreover, to build a 3D model of the PWR reactor core that we use as a reference calculation.

Serpent and Helios outputs are converted to the PMAXS format used by PARCS using GenPMAXS code [16].

### 4. HOMOGENIZED CROSS-SECTION DATA SETS GENERATION

In this section we highlight the details of the homogenized cross-section data generation. As described earlier, these data are produced using the deterministic lattice physics code Helios and the Monte Carlo code Serpent.

For Helios, the 190 energy group library based on ENDF/B-VI data files is used. The Serpent calculation is made using the continuous energy ACE format cross-section library based on ENDF/B-VI data files is used. One billion neutron histories are simulated. The B1 methodology is adopted in order to obtain cross-sections consistent with Helios.

The thermal cutoff energy for both calculations is 0.625 eV. Five different cross-section data sets are generated taking into account the configuration of the core, as described in Table III.

Table III. Generated cross section data sets

Identifier	Assembly type	Helios boundary conditions	Serpent boundary conditions
ASS1A	Fuel assembly without burnable absorbers and without spacer grids	All reflective	All reflective
ASS1B	Fuel assembly without burnable absorbers and with spacer grids	All reflective	All reflective
ASS2A	Fuel assembly with burnable absorbers and without spacer grids	All reflective	All reflective
ASS2B	Fuel assembly with burnable absorbers and with spacer grids	All reflective	All reflective
ASS3	Reflector	Reflective on N, S and W boundaries. Black on E boundary	Reflective on y-direction. Black on x-direction

Fig. 3 and Fig. 4 show the assembly models built with Helios taking advantage of the 1/8 symmetry. In order to take into account the presence of the spacer grids, the moderator material in ASS1B and ASS2B is replaced with a homogeneous mixture of H<sub>2</sub>O and Inconel-718, preserving the mass of the components. Material colors are for illustrative purposes.

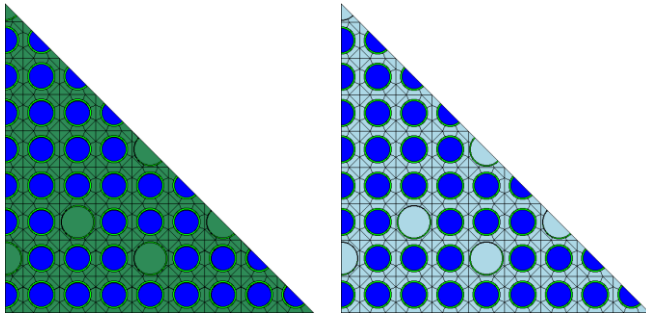


Fig. 3. ASS1A and ASS1B, Helios models

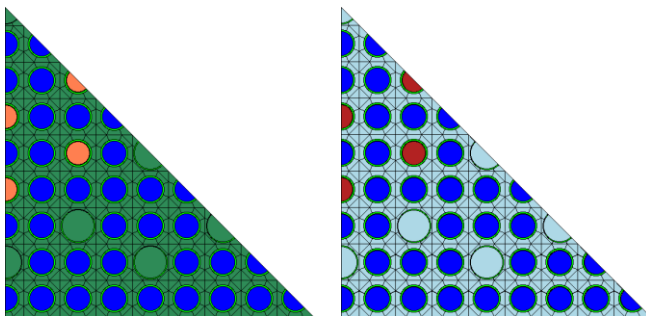


Fig. 4. ASS2A and ASS2B, Helios models

The Serpent fuel assembly models are built using the same geometry and material composition as Helios. However, the Serpent and Helios reflector model are different. Helios can set different boundary conditions on each side, while Serpent can only set different boundaries in the x, y and z-directions. Consequently, the Helios model for ASS3 is made of a fuel assembly and a reflector region.

Reflective boundary conditions are used on the North, South and West sides while black boundary conditions are used on the East side. The ASS3 Helios model is shown in Fig. 5.

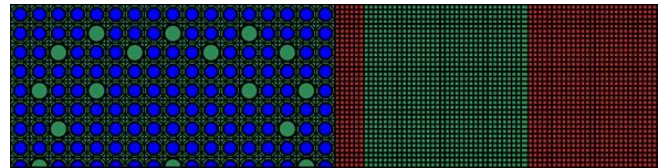


Fig. 5. ASS3, Helios model.

Considering the different boundary condition options, the Serpent model for ASS3 is made of 2 fuel assemblies surrounded by 2 reflector regions in the x-direction. Reflective boundary conditions are used in the y-direction while black boundary conditions are used in the x-direction. The ASS3 Serpent model is shown in Fig. 6.

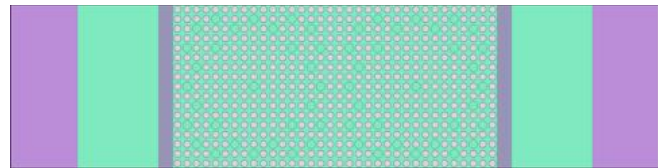


Fig. 6. ASS3, Serpent model

In both cases the cross-sections are homogenized in the reflector region only (baffle, moderator and thermal shield).

The above models were used to generate two-group diffusion parameters for PARCS.

Tables IV and V show the comparison between Helios and Serpent two-group diffusion parameters for the fuel assemblies. Tables IV and V reveal a very good agreement between the Helios and Serpent two-group constants. The most significant differences occur in the  $D_2$  and  $ADF_2$  calculations, where the Serpent results are approximately 2% higher than Helios. Table VI shows the comparison between Helios and Serpent two-group constants for the reflector.

Table IV. Comparison of homogenized diffusion parameters, ASS1A and ASS1B

Parameter	ASS1A		ASS1B	
	Helios	Serpent – Helios relative difference	Helios	Serpent – Helios relative difference
$D_1$	1.403E+00	0.33%	1.343E+00	0.49%
$D_2$	3.820E-01	2.25%	3.887E-01	1.76%
$\Sigma_{a,1}$	9.249E-03	0.60%	9.842E-03	0.61%
$\Sigma_{a,2}$	9.440E-02	-0.35%	1.025E-01	-0.38%
$\nu\Sigma_{f,1}$	7.608E-03	-0.76%	7.523E-03	-0.76%
$\nu\Sigma_{f,2}$	1.660E-01	-0.64%	1.616E-01	-0.64%
$\Sigma_{s,2 \leftarrow 1}$	1.651E-02	0.93%	1.504E-02	0.78%
$\Sigma_{s,1 \leftarrow 2}$	1.524E-03	-0.60%	1.837E-03	0.65%
$ADF_1$	1.000E+00	-0.25%	9.997E-01	-0.22%
$ADF_2$	9.993E-01	2.10%	1.000E+00	2.10%

Table V. Comparison of homogenized diffusion parameters, ASS2A and ASS2B

Parameter	ASS2A		ASS2B	
	Helios	Serpent – Helios relative difference	Helios	Serpent – Helios relative difference
$D_1$	1.439E+00	0.28%	1.373E+00	0.48%
$D_2$	3.818E-01	2.20%	3.879E-01	1.73%
$\Sigma_{a,1}$	9.642E-03	0.55%	1.023E-02	0.53%
$\Sigma_{a,2}$	1.040E-01	-0.14%	1.123E-01	-0.20%
$\nu\Sigma_{f,1}$	7.154E-03	-0.75%	7.063E-03	-0.76%
$\nu\Sigma_{f,2}$	1.555E-01	-0.65%	1.512E-01	-0.67%
$\Sigma_{s,2 \leftarrow 1}$	1.686E-02	1.00%	1.528E-02	0.83%
$\Sigma_{s,1 \leftarrow 2}$	1.614E-03	-0.29%	1.937E-03	0.96%
$ADF_1$	1.038E+00	0.49%	1.035E+00	0.41%
$ADF_2$	1.114E+00	2.24%	1.111E+00	2.19%

Table VI. Comparison of homogenized diffusion parameters, ASS3

Parameter	Helios	Serpent – Helios relative difference
$D_1$	1.263E+00	-0.17%
$D_2$	2.449E-01	4.21%
$\Sigma_{a,1}$	2.161E-03	-1.55%
$\Sigma_{a,2}$	2.389E-02	-0.93%
$\Sigma_{s,2 \leftarrow 1}$	2.505E-02	12.14%
$\Sigma_{s,1 \leftarrow 2}$	4.609E-04	-4.25%
$ADF_1$	1.084E+00	3.37%
$ADF_2$	2.525E-01	0.62%

Discrepancies in the two-group diffusion parameters are more significant in the reflector region than in the fuel assemblies. In particular, for  $\Sigma_{s, 2 \leftarrow 1}$  the Serpent results are approximately 12% higher the Helios. The reason for these changes is due to the difference in deterministic and Monte Carlo transport solution in large scattering regions.

### 5. FULL CORE ANALYSIS

The homogenized cross-section data generated by Helios and Serpent were converted in PMAXS format using GenPMAXS and used as an input for the nodal diffusion core simulator PARCS.

No thermal-hydraulics feedback is considered in this work. Fixed thermal-hydraulics conditions are considered and the calculation is performed assuming the core is at a constant temperature of 600 K. In all analyses, control rods are considered to be fully withdrawn. In addition, a 3D model of the PWR reactor, already shown in Figs. 1 and 2, is built with Serpent as a reference solution and run with five billion neutron histories.

The  $k_{eff}$  of the full core calculation is shown in Table VII. Figs. 7 and 8 show the comparison of the core radial power distribution and the relative differences, respectively. Fig. 9 shows the comparison of the axial power distribution in the three calculations.

Table VII. Comparison of the core  $k_{eff}$

Calculation sequence	$k_{eff}$	Deviation from reference (pcm)
Reference Serpent full core	$1.08847 \pm 0.00002$	-
PARCS/Helios	1.09018	144
PARCS/Serpent	1.08228	-526

0.786	1.138	0.786
1.138	1.305	1.138
0.786	1.138	0.786

a) PARCS/Helios

0.787	1.139	0.787
1.139	1.297	1.139
0.787	1.139	0.787

b) PARCS/Serpent

0.797	1.135	0.797
1.135	1.272	1.135
0.797	1.135	0.797

c) Reference Serpent full core

Fig. 7. Comparison of the core radial power distribution

-1.41	0.28	-1.44
0.30	2.56	0.26
-1.41	0.29	-1.43

a) PARCS/Helios vs. Reference Serpent full core

-1.31	0.38	-1.34
0.40	1.94	0.37
-1.31	0.40	-1.33

b) PARCS/Serpent vs. Reference Serpent full core

-0.10	-0.11	-0.10
-0.11	0.61	-0.11
-0.10	-0.11	-0.10

c) PARCS/Helios vs. PARCS/Serpent

Fig. 8. Relative differences (%) of radial power distribution

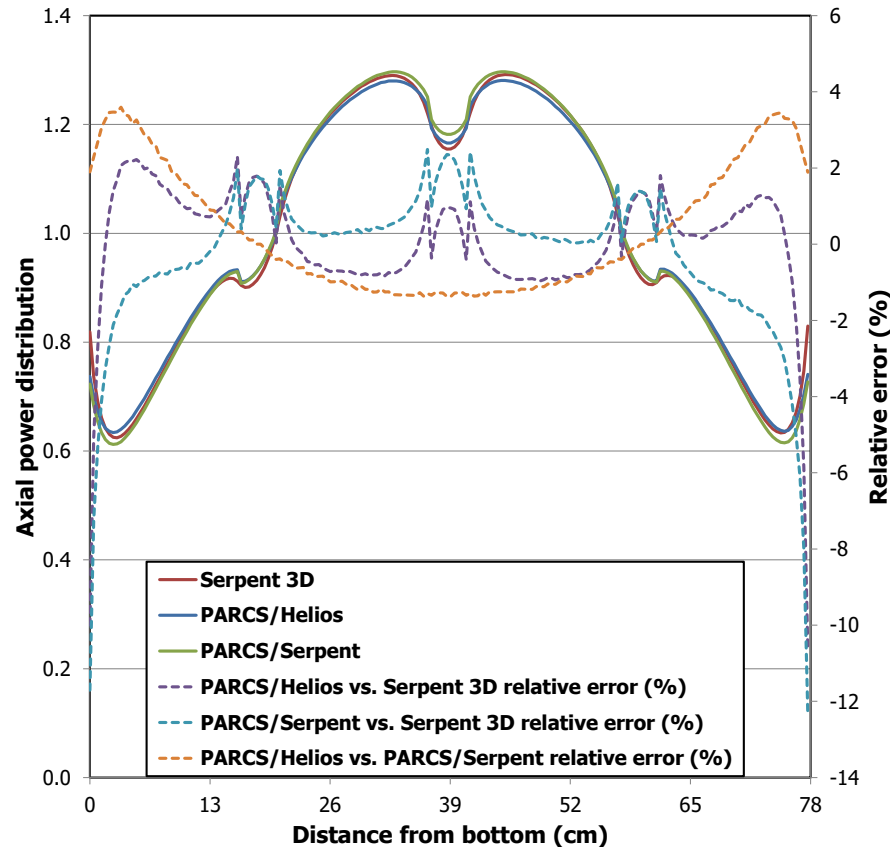


Fig. 9. Comparison of the axial power distribution

The results of the PARCS/Helios sequence are in a good agreement with the reference 3D Serpent calculation, even for such extremely small, high leakage core. The  $k_{\text{eff}}$  difference is less than 150 pcm. The most significant difference in radial power distribution is approximately 2.5%, for the central assembly.

The PARCS/Serpent results are also in a reasonably good agreement with the reference calculation. The  $k_{\text{eff}}$  difference is about 500 pcm. The most significant difference in radial power distribution is approximately 2%, again for the central assembly.

Regarding the axial power distribution, the power dips correspond to the spacer grids locations. The reference Serpent 3D axial power shape is well predicted by the PARCS/Helios and PARCS/Serpent calculations, considering that the relative error is below 2.5% in the majority of the core, except at the very periphery.

In general, the observed differences between PARCS and Serpent 3D are considered to be acceptable due to the small size of the core analyzed here. In such a core, the neutron spectrum varies strongly and the leakage effect is significantly more important than in a full scale PWR core or even an SMR. In order to capture such effects, the two-group energy structure used in this study may be not enough.

As already shown in [17], an increase in the number of energy groups may lead to better results.

## 5. CONCLUSIONS

The objective of this study was to provide details of the methodology of homogenized constant generation, to compare the results of deterministic and Monte Carlo lattice physics code (i.e. Helios and Serpent) and to validate the full core results obtained with a nodal code (i.e. PARCS) against a full-core Monte Carlo model. This analysis was performed with a very challenging small PWR core. Moreover, the effect of spacer grids on the neutronics core parameters, in particular the axial power distribution, was investigated.

Helios and Serpent homogenized cross-section data have shown to be in a good agreement, even if the two-group homogenized cross-sections in the reflector regions have shown differences that should be addressed.

Full-core calculations have shown a good agreement concerning  $k_{\text{eff}}$ , radial and axial power distribution. The PARCS/Helios results were in a good agreement with the reference 3D Serpent calculation, considering that the  $k_{\text{eff}}$  difference was less than 150 pcm and the largest difference

in radial power distribution was approximately 2.5%. Additionally, the PARCS/Serpent results were in a reasonably good agreement with the reference. In this case the relative difference of  $k_{\text{eff}}$  was approximately 500 pcm and the largest difference in radial power distribution was less than 2%. The most significant difference in the radial power distribution occurred in the central assembly. PARCS correctly predicts the shape of the axial power distribution, including the magnitude of power depression in the spacer grid locations. Relative errors were found to be below 2.5% in the majority of the core, except in the very periphery, next to the fuel-reflector interface, which is notoriously difficult for the nodal diffusion methods.

## REFERENCES

1. D.G. CACUCI et al., *Handbook of Nuclear Engineering*, Springer (2010).
2. E. FRIDMAN, J. LEPPÄNEN, “On the use of the Serpent Monte Carlo code for few-group cross section generation”, *Ann. Nucl. Energy* **38**, 1399–1405 (2011).
3. E. FRIDMAN, J. LEPPÄNEN, “On the use of the Serpent Monte Carlo code for few-group cross section generation”, *Ann. Nucl. Energy* **38**, 1399–1405 (2011).
4. M. HURSIN, A. VASILIEV, H. FERROUKHI, A. PAUTZ, “Comparison of Serpent and CASMO-5M for Pressurized Water Reactors models”, *International Conference on Mathematics and Computational Methods Applied to Nuclear Science & Engineering (M&C 2013)*, Sun Valley, ID, May 5-9 (2013).
5. D. J. SIEFMAN, G. GIRARDIN, A. RAIS, A. PAUTZ, M. HURSIN, “Full Core modeling techniques for research reactors with irregular geometries using Serpent and PARCS applied to the CROCUS reactor”, *Ann. Nucl. Energy* **85**, 434-443 (2015).
6. J. LEPPÄNEN, R. MATTILA, M. PUSA, “Validation of the Serpent-ARES code sequence using the MIT BEAVRS benchmark – Initial core at HZP conditions”, *Ann. Nucl. Energy* **69**, 212-225 (2014).
7. J. LEPPÄNEN, R. MATTILA, “Study on computational performance in generation of cross sections for nodal simulators using continuous-energy Monte Carlo calculations”, *Journal of Nuclear Science and Technology* **52**:7-8, 945-952 (2015).
8. E. FRIDMAN, S. DUERIGEN, Y. BILODID, D. KOTLYAR, E. SHWAGERAUS, “Axial discontinuity factors for the nodal diffusion analysis of high conversion BWR cores”, *Ann. Nucl. Energy* **62**, 129-136 (2013).
9. E. NIKITIN, E. FRIDMAN, K. MIKITYUK, “Solution of the OECD/NEA neutronic SFR benchmark with Serpent-DYN3D and Serpent-PARCS code systems”, *Ann. Nucl. Energy* **75**, 492-497 (2015).
10. E. FRIDMAN, E. SHWAGERAUS, “Modeling of SFR cores with Serpent–DYN3D codes sequence”, *Ann. Nucl. Energy* **53**, 354-363 (2013).
11. R. RACHAMIN, C. WEMPLE, E. FRIDMAN, “Neutronic analysis of SFR core with HELIOS-2, Serpent, and DYN3D codes”, *Ann. Nucl. Energy* **55**, 194-204 (2013).
12. J. BOUSQUET, A. SEUBERT, K. VELKOV, F.-P. WEISS, “Neutronic Modeling of the MYRRHA Minimum Critical Core with PARCS and Serpent”, *PHYSOR 2016*, Sun Valley, ID, May 1-5 (2016).
13. T. DOWNAR, Y. XU, T. KOZLOWSKI, D. CARLSON, “PARCS n2.7 US NRC Core Neutronics Simulator”, School of Nuclear Engineering, Purdue University W. Lafayette, Indiana, (2006).
14. R. J. STAMMLER, “Helios Methods”, Studsvik Scandpower, (2009).
15. J. LEPPÄNEN, et al, “The Serpent Monte Carlo code: Status, development and applications in 2013”, *Ann. Nucl. Energy*, **82**, 142-150 (2015).
16. A. WARD, Y. XU, T. DOWNAR, “GenPMAXS – v6.1.3”, University of Michigan (2015).
17. A. ROSENKRANTZ, M. AVRAMOVA, K. IVANOV, R. PRINSLOO D. BOTES, K. ELSAKHAWY, “Coupled 3D neutronics/thermal hydraulics modeling of the SAFARI-1 MTR”, *Ann. Nucl. Energy* **73**, 122-130 (2014).